Pflugers Arch - Eur J Physiol (2009) 457:1049–1060
DOI 10.1007/s00424-008-0575-5

Complex modulation of L-type Ca^{2+} current inactivation by sorcin in isolated rabbit cardiomyocytes

Mark R. Fowler · Gianni Colotti · Emilia Chiancone · Yoshiharu Higuchi · Tim Seidler · Godfrey L. Smith

Received: 8 June 2008 / Revised: 10 July 2008 / Accepted: 6 August 2008 / Published online: 2 September 2008

Abstract Modulation of the L-type Ca^{2+} channel (LTCC) by sorcin was investigated by measuring the L-type Ca^{2+} current ($I_{Ca,L}$) in isolated rabbit ventricular myocytes using ruptured patch, single electrode voltage clamp in the absence of extracellular Na^{+}. Fifty millimolars EGTA (170 nM Ca^{2+}) in the pipette solution buffered bulk cytoplasmic [Ca^{2+}], but retained rapid Ca^{2+}-dependant inactivation of $I_{Ca,L,}$. Recombinant sorcin (3 μM) in the pipette significantly slowed time-dependant inactivation (τ_{fast}: 8.8±0.9 vs. 15.1±1.7 ms). Sorcin had no significant effect on $I_{Ca,L,}$ after inhibition of the sarcoplasmic reticulum (SR). Using 10 mM 1,2-bis(*o*-*N*, *N*,*N*′,*N*′-tetraacetic acid (170 nM Ca^{2+}), $I_{Ca,L}$ inactivation was then determined by a Ca^{2+} -independent, voltage-dependant process. Under these conditions, 3 μM sorcin speeded up inactivation. A similar effect was observed by substitution of Ca^{2+} with Ba^{2+}. Down-regulation of endogenous sorcin to 27±7% using an RNAi adenoviral vector slowed inactivation of $I_{Ca,L}$ by ~42%. The effects of sorcin on voltage-dependant inactivation were mimicked by a truncated form of the protein containing only the Ca^{2+}-binding domain. This data is consistent with two independent actions of sorcin on the LTCC: (1) slowing Ca^{2+}-dependant inactivation and (2) stimulating voltage-dependant inactivation. The net effect of sorcin on the time-dependent inactivation of $I_{Ca,L}$ was a balance between these two effects. Under normal conditions, sorcin slows $I_{Ca,L}$ inactivation because the effects of Ca^{2+}-dependant inactivation out-weigh the effects on voltage-dependant inactivation.

Keywords Cardiac myocytes · Excitation–contraction coupling · Intracellular calcium · Ca^{2+} current · Inactivation · Membrane current

M. R. Fowler
Faculty of Biomedical & Life Sciences, University of Glasgow, Glasgow, UK

G. Colotti · E. Chiancone
Instituto di Biologia e Patologia Molecolari CNR, Dipartimento di Scienze Biochimiche, Universita La Sapienza, Rome, Italy

Y. Higuchi · T. Seidler
Department of Cardiology and Pneumology, Georg-August-University Goettingen, D-37075 Goettingen, Germany

G. L. Smith (✉)
Faculty of Biomedical & Life Sciences, West Medical Building, Level 4, Glasgow G12 8QQ, UK
e-mail: g.smith@bio.gla.ac.uk

Introduction

Sorcin is a 21.6-KDa intracellular Ca^{2+}-binding protein that is expressed in a variety of mammalian tissues including the heart [1–3], where it appears close to the transverse-tubular membrane system [3]. Sorcin has been shown to bind to two intracellular targets involved in excitation–contraction (E-C) coupling; the ryanodine receptor (RyR2) and the α_{1C}-subunit of the L-type Ca channel (LTCC) [3, 4]. Functionally, sorcin has been shown to reduce the activity of RyR2 [5, 6] and enhance inactivation of $I_{Ca,L}$ [7]. Effects on the activity of the Na/Ca exchanger (NCX) [6, 8] and the sarcoplasmic reticulum Ca^{2+}-ATPase (SERCA) [9] have also been reported. However, the effect of sorcin on the LTCC in myocardium is uncertain, since two studies have failed to demonstrate an effect [5, 6]. One complicating factor in studies on intact heart cells is that sorcin affects the activity of two proteins, the LTCC and RyR2, which are in close proximity at the interface between the T-tubule and

SR membranes. This area, known as the junctional cleft is a microdomain (10–20 nm wide [10, 11]) in which the diffusion of Ca^{2+} is restricted [12]. Ca^{2+} fluxes via LTCC and RyR2 influence the [Ca^{2+}] in the cleft, which in return regulates the activity of these proteins. In the case of the LTCC [Ca^{2+}], the cleft regulates the decay of $I_{Ca,L}$ via a Ca^{2+}-dependent inactivation (CDI) process [13–15]. An additional complication in distinguishing sorcin's action on the LTCC comes from the recent evidence that the activity of NCX can affect CDI by influencing the [Ca^{2+}] within the cleft [16]. Therefore, sorcin's apparently variable action on the LTCC may arise from parallel effects on NCX and the SR of cardiac muscle. To test this hypothesis, the present study used Na^+- and K^+-free solutions in combination with high intracellular concentrations of Ca^{2+} buffers. The data revealed for the first time two independent and functionally opposing effects on CDI and voltage-dependent/Ca^{2+} independent inactivation (CII/VDI).

Materials and methods

Isolation of rabbit ventricular myocytes

New Zealand White rabbits (2–2.5 kg) were euthanized by administration of an intravenous injection of 500 IU heparin together with an overdose of sodium pentobarbitone (100 mg kg^{-1}). Hearts were removed in accordance with the United Kingdom Animals (Scientific Procedures) Act 1986, and the Guide for the Care and use of Laboratory Animals published by the US National Institutes of Health (NIH Publication No. 85-23, revised 1985). Ventricular cardiomyocytes were then isolated as previously described [17] and suspended in Krebs buffer of the following composition (mM): NaCl, 140; KCl, 4; $MgCl_2$, 1; $CaCl_2$, 1; glucose, 11.1; HEPES, 5; pH 7.4, Ca^{2+} 1.8 mM.

Electrophysiology

Ventricular myocytes were whole cell voltage clamped using an Axon Axoclamp 2B switch clamp amplifier in discontinuous mode (10–35 kHz); voltage and current signals were filtered at 1 kHz. Patch electrodes had a resistance of 2–10 MΩ when back filled with the internal solution described below. Following patch rupture and dialysis (5 min), $I_{Ca,L}$ was elicited by a 300-ms step depolarization from –40 to 0 mV, preceded by a 50-ms prepulse from –80 to –40 mV to inactivate I_{Na} at 0.5 Hz.. Current–voltage relations were obtained by depolarizing the cell to a range of test pulses between –40 and +80 mV in 10 mV increments. Steady-state voltage-dependent activation and inactivation was assessed by a double pulse protocol where a test pulse to 0 mV was preceded by a range of conditioning pulses between –60 and +60 mV in 10 mV steps at 0.5 Hz. Experiments examining $I_{Ca,L}$ in adult cardiomyocytes cultured for 96 h used a depolarizing step to +20 mV.

Pipette and extracellular solutions

The pipette solution contained (in mM): Cs_2EGTA, (0.01–50); CsCl, 20; TEACl, 35; $MgCl_2$, 4.5; Na_2ATP, 4; Na_2CRP, 1; HEPES, 20; Ca, 25 (free Ca^{2+}, 170±5 nM, n=10). To achieve the range of [EGTA] described in the solution above, a near identical pipette solution was made with the following composition (in mM): CsCl, 120; TEACl, 35; $MgCl_2$, 4.5; Na_2ATP, 4; Na_2CRP, 1; HEPES, 20; EGTA, 0.3; pH 7.25 with CsOH. Ca^{2+} concentration was titrated to equal that of the 50 mM solution (calculated to be 170 nM) with $CaCl_2$ using a spectrophotometer and Fura 2 (free acid, Molecular Probes). These two solutions could then be mixed as desired to yield intracellular solutions with identical Ca^{2+} activities but with varying [EGTA].

Where required, 1,2-bis(*o*-ethane-*N*,*N*,*N*′,*N*′-tetraacetic acid (BAPTA; 10 mM) was added to the pipette solution and free Ca^{2+} activity corrected by the addition of Ca^{2+} (from a 100-mM $CaCl_2$ stock). Free [Ca^{2+}] was calculated as described [18] and checked using Fura-2 fluorescence in a cuvette-based spectrophotometer system. Extracellular solutions devoid of Na^+ and K^+ were based on previous studies [19] (in mM): TEACl, 140; CsCl, 4; HEPES, 5; $MgCl_2$, 1; $CaCl_2$, 1.8; Glucose, 11.1; 4AP, 5; pH to 7.4 with CsOH. The osmolarity of both intracellular and extracellular solutions did not vary by more than 5%.

Intracellular [Ca^{2+}]

Monitoring of intracellular Ca^{2+} (Ca^{2+}_i) was performed using Fura-2 (100 μM), introduced into the cell via the patch pipette, and the fluorescence was monitored using a Cairn monochrometer (Carin, Faversham, Kent, UK).

Expression and purification of wild-type sorcin and its variants

Chinese hamster ovary recombinant sorcin was expressed in *E. coli* BL21 (DE3) cells and purified as previously described [20]. The same purification procedure was used for the truncated protein. Protein concentration was determined spectrophotometrically at 280 nm. Full-length sorcin and the truncated peptide consisting of the C-terminus only [sorcin–calcium-binding domain—(SCBD)] was added to the intracellular pipette solution for dialysis into the cell at a concentration of 3 μM using a protocol

similar to previous work [5]. Allowing sorcin to dialyze into the cell for up to 10 min had no additional effects (data not shown). Preliminary experiments using 1 μM sorcin had no significant effect on the L-type Ca^{2+} current. The absence of significant changes in $I_{Ca,L}$ over the duration of the experiment (10–15 min) suggests that loss of endogenous sorcin from the cardiomyocytes by dialysis via the pipette was of minor consideration.

Preparation and testing of RNAi virus

A partial rabbit sorcin sequence was amplified using primers based on the known human sorcin sequence by reverse transcription of RNA from a chinchilla bastard rabbit. Sense and antisense oligonucleotides were chosen to target the 19 nucleotide (nt) segment complementary to the rabbit sorcin mRNA sequence GCAAGAUCACCUUCGAUGA and ligated downstream of a U6 promoter into vector pSIREN-DNR (BD Biosciences Clontec, Palo Alto, USA). Recombination with the remaining adenoviral genome using pAdeno-X vector was carried out according to manufacturers instructions (BD Adeno-X Expression System, BD, Biosciences Clontec, Palo Alto, CA, USA) and virus upscaling and purification was undertaken as described before [6].

Adenoviral infection with a multiplicity of infection of 100 was performed to produce 2 populations of adenovirus-transfected cardiomyocytes: (1) expressing the Sorcin RNAi (Ad-SorRNAi) and (2) expressing β-galactosidase as control (Ad-LacZ). Infected cardiomyocytes were subsequently cultured in supplemented medium M199 (Sigma) for 96 h. Western blot analysis indicated the level of down-regulation to be 0.27±0.7 (n=5, P<0.05) of that in Ad-LacZ transfected cells (Fig. 5).

Immunoblotting used the NuPAGE system (Invitrogen) with 10% Bis–Tris gels and MOPS buffer. CSQ in cell lysates from Ad-LacZ and Ad-Sorcin-RNAi transfected cells was detected with mouse monoclonal anti-CSQ at 1:200 dilution. CSQ protein levels in both experimental groups were used as a standard. Sorcin antibody (rabbit polyclonal, a kind gift from Dr. Valdivia, Madison, WI, USA) was used at 1:10,000 dilution. Immunoblots were quantified using image analysis software (Quantity One, BioRad)

Data analysis and statistics

Peak $I_{Ca,L}$ was taken as the difference current between the current peak and steady state at the end of the test voltage pulse and is expressed as a function of cellular capacitance. $I_{Ca,L}$ CDI is evident as a Ca^{2+}-dependent inactivation best described by a double exponential function fitted to the decay phase of the current [19].

A measure of the Ca^{2+} buffering imposed by EGTA and BAPTA within the cell was gained using the following equation: length constant of buffer $= \sqrt{(D_{Ca}/K_{on} \cdot B_T)}$ [21], where D_{Ca} is the diffusion of Ca^{2+} in the cytosol, K_{on} is the rate of Ca^{2+} binding by the buffer and B_T is the buffer concentration. Estimates of the equation constants were taken from Soeller and Cannell and Naraghi and Neher [21, 22]. The length constants are described in the relevant sections. Data were statistically analyzed using unpaired t tests or one-way analysis of variance (ANOVA), with interactions where appropriate using Sigma Stat (Jandel Scientific), and significance was taken at 5%.

Results

Retention of CDI despite buffering of bulk cytoplasmic Ca^{2+}

Figure 1a illustrates the lack of significant changes in $I_{Ca,L}$ (amplitude and inactivation see inset) and the progressive decrease in the amplitude of the Ca^{2+} transient as the [EGTA] in the patch pipette is progressively increased ($[Ca^{2+}]$ ~170 nM). At 50 mM EGTA, there was no detectable change in bulk intracellular $[Ca^{2+}]$. Figure 1b shows the mean values of amplitude and rate of inactivation. Also shown for comparison are the mean values for $I_{Ca,L}$ amplitude and rate of inactivation recorded from cells with minimal EGTA (10 μM) in solutions containing normal Na^+ and K^+ (square symbols). Under these conditions (50 mM EGTA), Ca^{2+} influences LTCC in a spatially restricted region, and so the next series of experiments examined the modulatory influence of sorcin on $I_{Ca,L}$ in the absence of changes in bulk cytoplasmic $[Ca^{2+}]$.

The effect of sorcin on the time-dependant inactivation of $I_{Ca,L}$

As shown in Fig. 1c(i), the rate of inactivation of $I_{Ca,L}$ following a depolarizing step to 0 mV (0.5 Hz) was significantly slowed by the inclusion of sorcin in the pipette solution [τ_{fast} control 8.8±0.9 ms, n=14; τ_{fast} sorcin 15.1±1.7 ms, n=9, Fig. 1c(ii)]. Inactivation rate was not significantly altered following dialysis of the EGTA and TRIS-containing buffer used for the suspension of sorcin in the absence of the protein (τ_{fast} buffer 9.9±2.1 ms, n=4, vs. τ_{fast} control, 8.8±0.9 ms, n=14) or when sorcin was denatured by boiling for 5 min (10.9±0.9 ms, n=6, P>0.05 vs. control). Sorcin did not modulate the slow component of inactivation (τ_{slow}) which remained almost an order of magnitude larger than τ_{fast} as described previously [19] (τ_{slow} control 68.4±6 ms, n=14; sorcin, 71.1±15 ms, n=9,

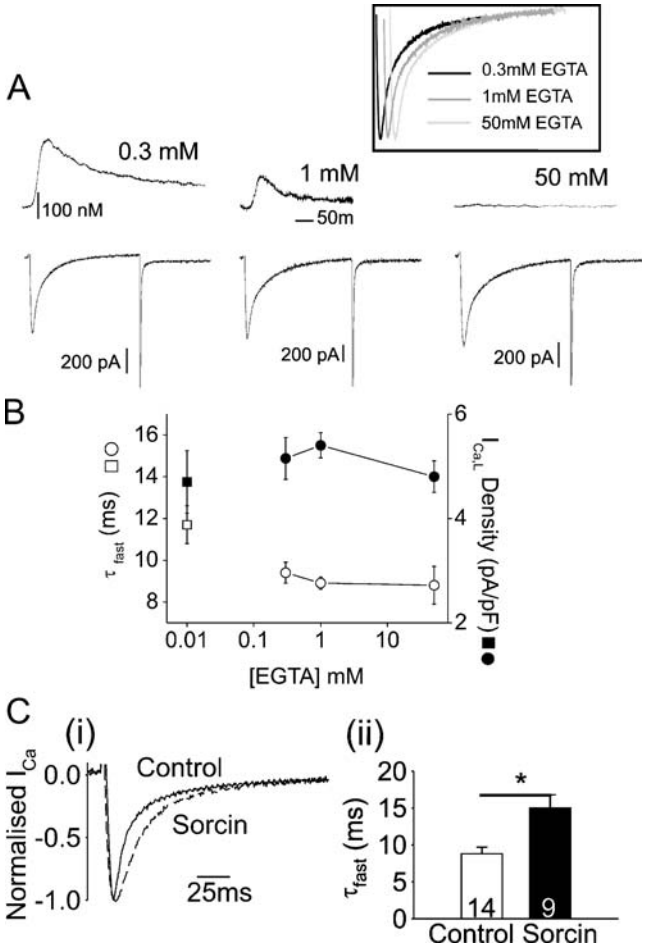

Fig. 1 The effect of sorcin on inactivation of $I_{Ca,L}$ in a highly Ca^{2+} buffered environment. **a** Specimen recordings of intracellular Ca^{2+} (*top panels*) and $I_{Ca,L}$ (*bottom panels*) at increasing [EGTA] from 0.3–50 mM. $I_{Ca,L}$ was elicited by step depolarization from –40 to 0 mV, this followed a 50-ms prepulse from –80 mV. *Inset* side-by-side comparison of the current inactivation profiles shown in **a**. **b** Mean data (±SEM) of τ_{fast} (*open circles*) and current density (*closed circles*) to increases in [EGTA]. The *open* and *closed squares* indicate τ_{fast} and current density respectively in an unbuffered cell (10 μM EGTA) for comparison. **c** *i–ii* Inactivation is sensitive to sorcin in the presence of 50 mM EGTA. *Numbers on bars* indicate numbers of cells. *Asterisk* indicates significant relationship at $P<0.05$ with unpaired *t* test

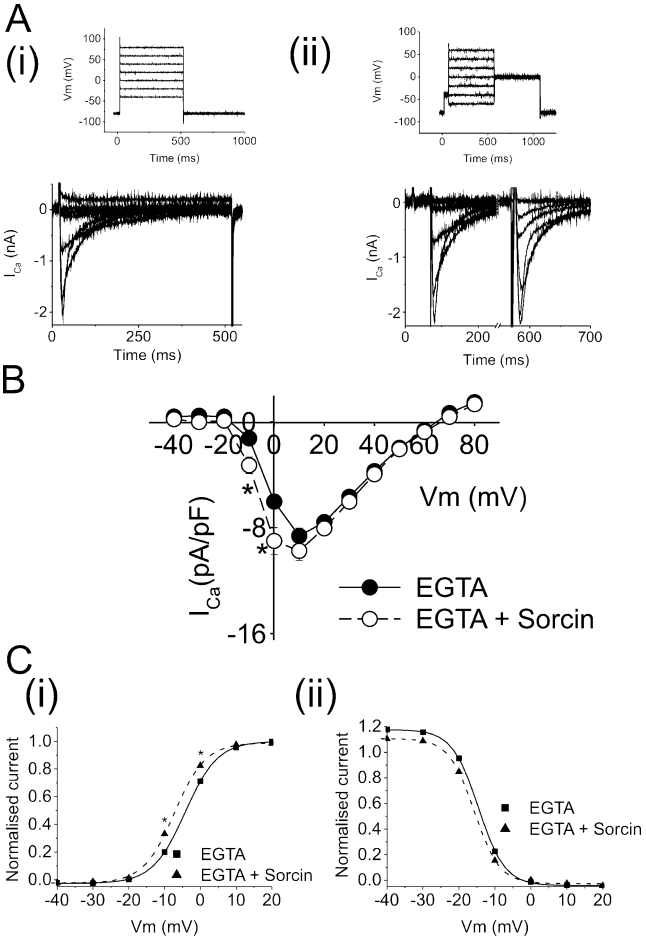

Fig. 2 Effect of sorcin on whole cell $I_{Ca,L}$ properties. **a** *i–ii* Voltage protocols (0.5 Hz) and current families generated from single and double pulse protocols. **b** Current–voltage (*I–V*) relation of $I_{Ca,L}$ in the presence of an EGTA-based pipette solution ($n=9$ for each group). **c** *i* Activation curves generated by the double pulse protocol shown in a *ii*, which illustrate the negative shift in activation voltage (V_{half}) in the presence of sorcin (see text for further details). **c** (ii) Inactivation curves were not sensitive to the presence of sorcin in the patch pipette. *Asterisk* indicates significant relationship at $P<0.05$ with unpaired *t* test

$P>0.05$). This effect of sorcin was also observed in a limited set of experiments where $I_{Ca,L}$ was elicited by a step depolarization from –80 to 0 mV (without the prepulse to –40 mV) in the absence of extracellular Na^+.

The effect of sorcin on the *I–V* relationship of $I_{Ca,L}$

Current voltage and steady-state current activation and inactivation relations were generated using the voltage protocols illustrated in Fig. 2a(i–ii). Sorcin increased peak current at −10 and 0 mV ($P<0.05$; Fig. 2b). The family of activation curves generated by the double pulse protocol indicates a negative shift in activation voltage (V_{half}) associated with sorcin, which was significantly different at –10 and 0 mV [$P<0.05$; Fig. 2c(i)]. Under control conditions, V_{half} was −4.2±0.08 mV, while in the presence of sorcin, activation was more negative (V_{half} was −7.3 mV± 0.02, $P<0.05$). The double pulse protocol also reveals the steady-state inactivation properties of $I_{Ca,L}$ which were not significantly altered at any of the test voltages [Fig. 2c(ii)]. It appears that the major effects of sorcin on macroscopic current properties are alterations to steady-state activation. However, since the rate of CDI is not altered at –10 and 0 mV, changes in current magnitude do not explain the effect of sorcin on the inactivation of $I_{Ca,L}$ [19]. The next series of experiments therefore examined potential mecha-

nisms for the modulatory influence of sorcin on the time-dependant inactivation of $I_{Ca,L}$.

The ability of sorcin to modulate inactivation of $I_{Ca,L}$ after inhibition of the SR

The activity of the SR was inhibited using thapsigargin (25 μM; 10 min) or ryanodine (30 μM; 10 min). Inhibition of the SR slowed inactivation of $I_{Ca,L}$ following a step depolarization to 0 mV [Fig. 3a(i–ii)]. Under these conditions, there was no significant modulation of $I_{Ca,L}$ by sorcin (Fig. 3b(i–ii). The loss of sorcin's action on $I_{Ca,L}$ after SR inhibition may be linked to diminished $[Ca^{2+}]$ release into the junctional cleft during activation. To test this hypothesis, Ca^{2+} entry through the LTCC was increased by elevating extracellular $[Ca^{2+}]$ to 5.4 and 20 mM Ca^{2+} in the presence of thapsigargin; this increased whole cell current from 6.0±0.5 pA/pF ($[Ca^{2+}]_o$=1.8 mM) to 18.4±5.8 pA/pF (n=5; P<0.05; $[Ca^{2+}]_o$=20 mM) Raising extracellular $[Ca^{2+}]$ resulted in faster inactivation despite the absence SR Ca^{2+} release (Fig. 3c black triangles). However, the rate of inactivation was not altered significantly by sorcin at 5.4 mM Ca^{2+} (step to 0 mV) or 20 mM Ca^{2+} (step to +10 mV, Fig. 3c open triangles). Sorcin was also without effect on inactivation at +20 mV with 20 mM extracellular Ca^{2+}. Data in the absence of thapsigargin is shown for comparison (open and filled circles). These data strongly suggest that sorcin activation requires the conditions prevalent in the junctional cleft/dyad. This was tested further by examining the effect of sorcin in the presence of the faster Ca^{2+} buffer BAPTA.

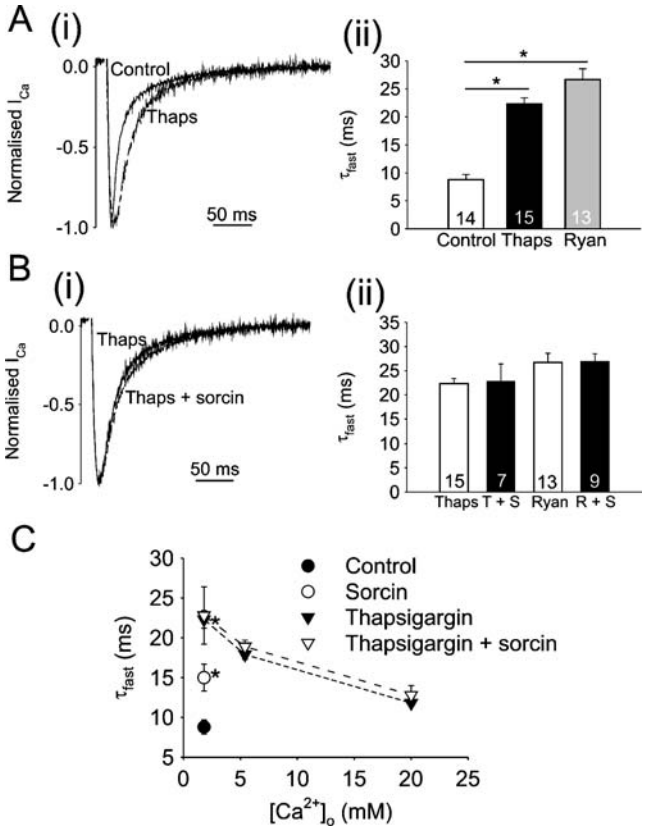

Fig. 3 SR inhibitors alter the effect of sorcin on inactivation of $I_{Ca,L}$. **a** *i–ii* Inhibition of the SR (thapsigargin, 25 μM or ryanodine, 30 μM) slows $I_{Ca,L}$ CDI to 22.3±1.1 ms (thapsigargin, n=15) and to 26.7±1.9 ms (ryanodine, n=13). **b** *i–ii* Sorcin had no effect on $I_{Ca,L}$ inactivation following SR inhibition with either thapsigargin (τ_{fast} thapsigargin, 22.3±1.1 ms, n=15; thapsigargin + sorcin 22.8±3.6 ms, n=7, P>0.05) or ryanodine (τ_{fast} ryanodine, 26.7±1.9 ms n=13; ryanodine + sorcin, 26.9±1.6 ms, n=9, P>0.05). **c** The effect of sorcin on inactivation of $I_{Ca,L}$ was not restored in the presence of SR inhibition by raising extracellular $[Ca^{2+}]$: 5.4 Ca^{2+}: 17.9±0.6 ms (n=8); 5.4 Ca^{2+} + sorcin: 18.9±0.8 ms (n=9), P>0.05; 20 Ca^{2+}: 11.8±0.3 ms (n=6); 20 Ca^{2+} + sorcin: 12.8±1.2 (n=6), P>0.05 (*open and closed inverted triangles*). Control data (±sorcin) in the absence of thapsigargin is shown for comparison at 1.8 mM Ca^{2+}(*circles*). *Asterisk* indicates significant relationship at P<0.05 with one-way ANOVA versus control

Sorcin's action on $I_{Ca,L}$ in the presence of BAPTA

In order to investigate the effects of sorcin on $I_{Ca,L}$ in the absence of Ca^{2+}-dependant inactivation, 10 mM BAPTA with identical diastolic Ca^{2+} to previous measurements (170 nM Ca^{2+}) was used in the patch pipette to further limit the rise in $[Ca^{2+}]$ in the microdomain. Calculations suggest that 10 mM BAPTA is capable of buffering intracellular Ca^{2+} at distances of ~7 nm [21]. In the presence of sorcin, τ_{fast} was significantly faster following a step depolarization to 0 mV [Fig. 4a(i–ii)]. In separate experiments, $I_{Ca,L}$ was elicited from a holding potential of –80 in 10 mV increments to a range of test pulses as described previously. In the presence of sorcin, peak current density was significantly larger at +10 mV (P<0.05; Fig. 4bi). The values of V_{half} for activation and inactivation were not significantly different [Fig. 4b(ii–iii)]. Separate experiments in the presence of BAPTA showed that inhibition of the SR had no further effect on inactivation rate (data not shown). These data therefore suggest that, in the presence of BAPTA (170 nM Ca^{2+}), sorcin has modest effects on the *I–V* relationship of $I_{Ca,L}$ but the rate of $I_{Ca,L}$ inactivation is significantly increased, in contrast to that observed in the presence of EGTA. To test whether this effect is due to minimizing Ca^{2+}-dependant inactivation by BAPTA, measurements were repeated using Ba^{2+} as the charge carrier.

Is a rise in sub-sarcolemmal Ca^{2+} a requirement for the action of sorcin on the LTCC?

To remove Ca^{2+} completely from the junctional cleft, 1.8 mM Ba^{2+} was substituted for Ca^{2+} in the extracellular

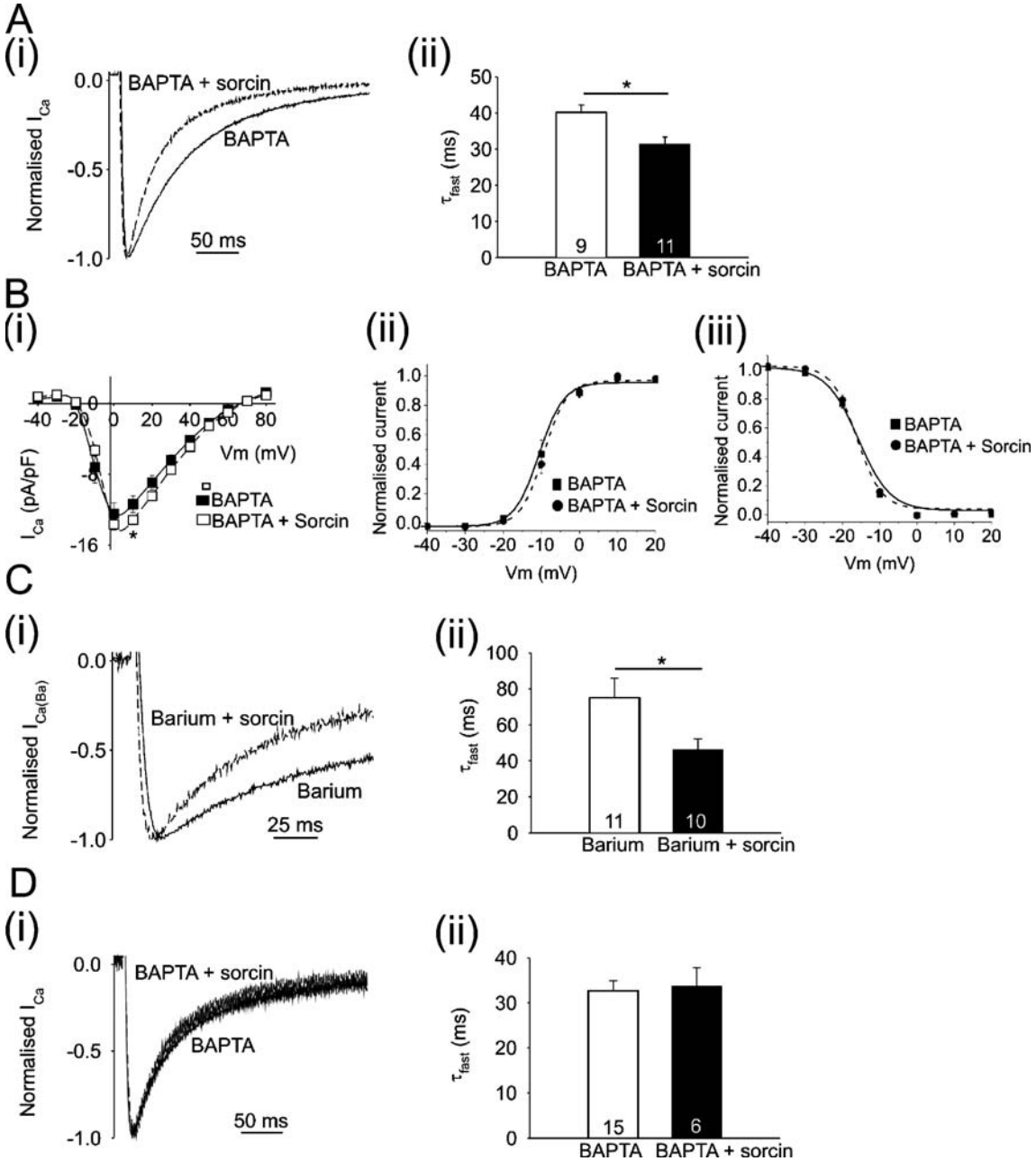

Fig. 4 Sorcin's action on $I_{Ca,L}$ in the presence of BAPTA. **a** *i–ii* CII/VDI was speeded up by the presence of sorcin in the patch pipette following a step depolarization to 0 mV (0.5 Hz). **b** *i I–V* relation in the presence and absence of sorcin with BAPTA in the patch pipette. Peak current was significantly larger at +10 mV ($P<0.05$). **b** *ii* Steady-state activation of $I_{Ca,L}$ with BAPTA in the pipette solution was not sensitive to the presence of sorcin. **b** *iii* Inactivation in the presence of BAPTA was also unaffected by sorcin in the patch pipette. **c** *i–ii* Sorcin speeded up voltage-dependent inactivation when extracellular Ca^{2+} was replaced by Ba^{2+}. **d** *i–ii* Sorcin was unable to mediate effects on inactivation of $I_{Ca,L}$ when Ca^{2+} in the junctional cleft was lowered to <1 nM

perfusate and $I_{Ca(Ba)}$ recorded using 50 mM EGTA (170 nM Ca^{2+}) in the patch pipette solution. Under these conditions, sorcin significantly increased the rate of inactivation [τ_{fast} control 75±11 ms, $n=11$; τ_{fast} sorcin 46.3±6 ms, $n=10$, $P<0.05$, Fig. 4c(i–ii)]. If BAPTA (10 mM) was added to the patch pipette without correction of free Ca^{2+}, the free [Ca^{2+}] in the patch pipette (and therefore within the cell) is reduced to <1 nM, and under these conditions, addition of sorcin did not significantly modulate current inactivation with a Ca^{2+}-containing extracellular perfusate [Fig. 4d(i–ii)], suggesting that sorcin was ineffective at modulating $I_{Ca,L}$ when cytoplasmic [Ca^{2+}] is below 1 nM.

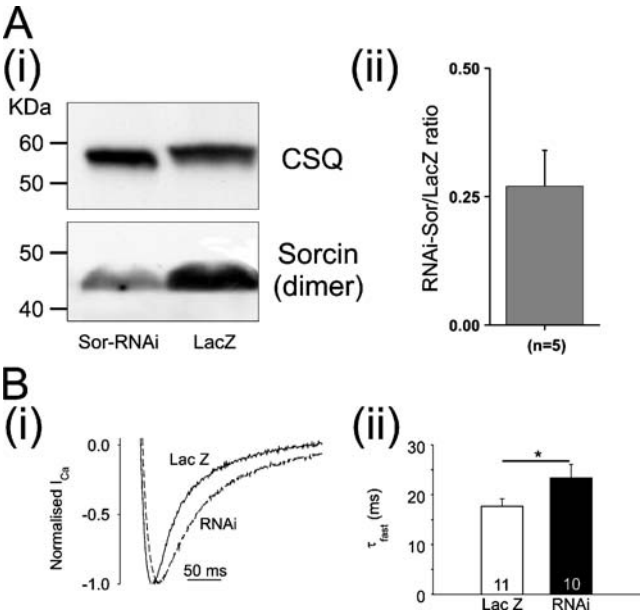

Fig. 5 Modulation of $I_{Ca,L}$ by sorcin down-regulation. Down-regulation of sorcin using an RNAi strategy (RNAi–Sor) significantly slowed CDI (BAPTA pipette solution 170 nM Ca^{2+}) compared to control (LacZ). **a** *i* a sample Western of sorcin dimer and the corresponding calsequestrin signal from cultured cardiac myocytes after transfection with RNAi for sorcin (RNAi–Sor) and the control virus (LacZ). **a** *ii* average data showing the significant down-regulation of sorcin (n=number of transfections) **b** *i–ii* Electrophysiological recordings of $I_{Ca,L}$ following a voltage step to +20 mV. τ_{fast} was significantly increased following sorcin down-regulation. *Numbers on bars* indicate number of cells. *Asterisk* indicates significant relationship at $P<0.05$ with unpaired t test

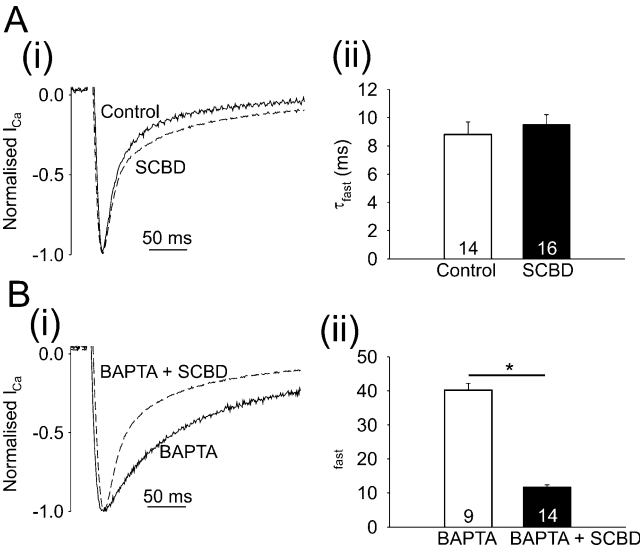

Fig. 6 Truncated sorcin modulates inactivation of $I_{Ca,L}$ with BAPTA in the patch pipette. **a** *i–ii* Inactivation kinetics were not significantly altered with 3 μM SCBD in the patch pipette under control conditions. **b** *i–ii* Current inactivation was enhanced by SCBD when inactivation of $I_{Ca,L}$ was measured in the presence of by BAPTA. *Numbers on bars* indicate number of cells. *Asterisk* indicates significant relationship at $P<0.05$ with unpaired t test

Does-endogenous sorcin modulate the LTCC?

An RNAi adenovirus construct was used to down-regulate native sorcin expression to 27±7% of control value in adult cultured cardiomyocytes [Fig. 5a(i–ii)]. Examination of $I_{Ca,L}$ (170 nM Ca^{2+}) showed that the rate of inactivation was significantly slowed compared to control [Ad-LacZ infected; Fig. 5b(i–ii)] indicating a modulatory role for endogenous sorcin.

Truncated construct of sorcin indicates C-terminal interaction with LTCC

Biochemical analysis has demonstrated key regions of the sorcin protein involved in the interaction with target proteins. Specifically, these sites are located at the C- and N-terminals of the protein [20]. We investigated the domain involved in interaction with $I_{Ca,L}$ using a truncated form of sorcin that contains only the C-terminus (sorcin–calcium-binding-domain, SCBD) [20]. Inclusion of SCBD in the patch pipette did not significantly alter current inactivation [Fig. 6a(i–ii)], but repeating these experiments in the presence of BAPTA (170 nM Ca^{2+}) resulted in a significant increase in the rate of current inactivation [Fig. 6b(i–ii)]. These results suggest that a C-terminus interaction dominates in the interaction with LTCC.

Are kinase pathways involved in the mechanism of action of sorcin on $I_{Ca,L}$?

We also considered whether sorcin influenced $I_{Ca,L}$ indirectly by affecting intracellular signaling pathways that alter $I_{Ca,L}$ by phosphorylation of LTCC. The two main kinases responsible are protein kinase A (PKA) and calcium–calmodulin-dependant kinase type II (CaMKII). CaMKII is thought to be responsible for mediating frequency-dependent facilitation (FDF) of $I_{Ca,L}$ [23], which is manifested by an increase in peak current and a slowing of inactivation as the frequency of contraction increases. From a holding potential of –80 mV, $I_{Ca,L}$ displayed facilitation following an increase in stimulation frequency from 0.1 to 1 Hz: inactivation kinetics were slowed on the fifth pulse at 1 Hz compared to the first pulse [Fig. 7a(i) and b], while current magnitude increased (the ratio of peak current at beat 5 compared to beat 1 (B5/B1) increased to 1.26± 0.02, n=8). Five micromolars of KN-93 (a CaMKII inhibitor) abolished the rate-dependent slowing of inactivation [Fig. 7a(ii) and b], while B5/B1 was decreased to 0.88± 0.02 (n=8). No significant effect of KN-93 was observed on $I_{Ca,L}$ density during facilitation. This data confirms the involvement of CaMKII in mediating facilitation of $I_{Ca,L}$ and provides evidence that KN-93 treatment was effectively

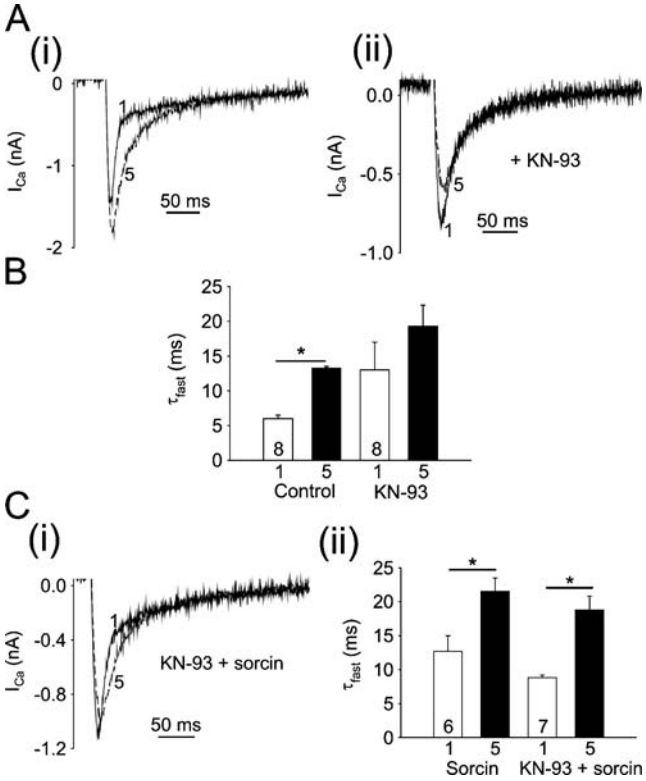

Fig. 7 CaMKII is not involved in modulation of $I_{Ca,L}$ by sorcin. **a** *i* τ_{fast} increased from 6±0.5 ms (beat 1, n=8) to 13.3±2 ms (beat 5, n=8, P< 0.05), following an increase in pacing frequency from 0.1 to 1 Hz (Fig. 6b, *left* pair of bars). **a** *ii* $I_{Ca,L}$ facilitation was abolished by the CaMKII inhibitor KN-93 (5 μM), since τ_{fast} was not significantly prolonged following an increase in pacing frequency (beat 1, 13.1± 3.7 ms, n=8; beat 5, 19.3±2.8 ms, n=8, P>0.05; Fig. 6b, *right* pair of bars). **c** *i–ii* In the presence of KN-93 τ_{fast} which increased from 8.8± 0.4 ms at beat 1 (n=7) to 18.8±2.2 ms at beat 5 (n=7) in the presence of sorcin (P<0.05). *Numbers on bars* indicate numbers of cells. *Numbers below bars* indicate beat number at higher stimulation frequency (1 Hz). *Asterisk* indicates significant relationship or significantly different from control, at P<0.05 with unpaired t test

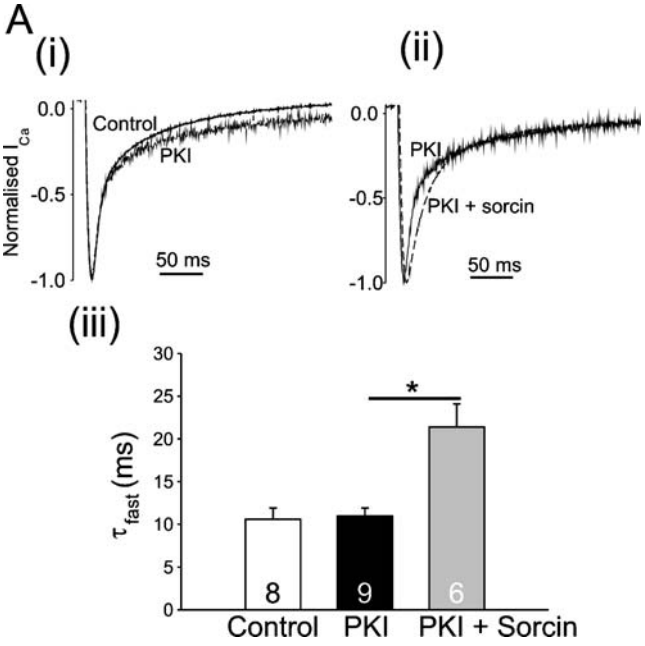

Fig. 8 PKA is not implicated in sorcin effect on I_{CaL}. **a** *i* Inhibiting PKA with PKI (10 μM) had no effect on current in the absence of sorcin. **a** *ii–iii* PKA inhibition does not influence the effect of sorcin on CDI. *Numbers on bars* indicate numbers of cells. *Asterisk* indicates significant relationship at P<0.05 with one-way ANOVA

blocking CaMKII activity. Under these conditions, sorcin-mediated changes in $I_{Ca,L}$ inactivation were not blocked by the presence of KN-93 [Fig. 7c(i–ii)], suggesting that inhibition of CaMKII does not influence the effect of sorcin on $I_{Ca,L}$ inactivation kinetics.

We also investigated the role of protein kinase A (PKA) using the inhibitory peptide (PKI). The inclusion of PKI in the patch pipette did not significantly affect the ability of sorcin to modulate inactivation of $I_{Ca,L}$ [Fig. 8a(i–iii)]. These data are consistent with sorcin's actions on $I_{Ca,L}$ without the involvement of CaMKII and PKA.

Discussion

This paper presents novel data describing the effects of sorcin on $I_{Ca,L}$ in rabbit ventricular myocytes. Sorcin (3 μM) increased $I_{Ca,L}$ over a limited range of voltages but had two distinct and opposing effects on the inactivation of $I_{Ca,L}$: (1) slowing the rate of CDI and (2) enhancing the rate of CII/VDI.

Is the modulation of $I_{Ca,L}$ by sorcin due to an effect on the *I–V* relationship?

The inclusion of sorcin in the patch pipette had small but significant effects on $I_{Ca,L}$ current–voltage relations consistent with a leftward shift in the activation curve of the current. In addition to the effects on the current–voltage relationship, sorcin had significant effects on the time course of activation, evident at 0 and +10 mV but not at −10 mV. These data and the previously published relationship between inactivation rates and voltage [19] indicate that the effect of sorcin on time-dependent inactivation is a distinct action and not a consequence of the changes in the current voltage relationship.

Modulation of CDI and VDI by sorcin

Sorcin's action on $I_{Ca,L}$ inactivation was observed when 50 mM EGTA was used to buffer cytoplasmic Ca^{2+}, indicating that a transient rise in bulk cytoplasmic [Ca^{2+}] was not required for modulation. The ability of sorcin to influence $I_{Ca,L}$ inactivation appeared to require a functional SR, since there was no apparent effect of sorcin after ryanodine or thapsigargin treatment. This would suggest

that the action of sorcin on the LTCC required the transiently high Ca^{2+} signal that exists within the junctional cleft as a result of SR Ca^{2+} release. However, the data in the presence of BAPTA would tend to argue against this. The more rapid buffering by BAPTA (170 nM Ca^{2+}), which limits the rise of Ca^{2+} in the junctional cleft results in much slower $I_{Ca,L}$ inactivation than was observed following SR inhibition. This is as expected if Ca^{2+}-dependent inactivation was substantially attenuated. This indicates that SR inhibition alone reduces but does not abolish Ca^{2+}-dependent inactivation, i.e., it does not abolish the increase in [Ca^{2+}] in the cleft. The slower inactivation of $I_{Ca,L}$ in the presence of 10 mM BAPTA was unaffected by SR inhibition (data not shown) indicating that 10 mM BAPTA was capable of preventing SR Ca^{2+} release from influencing cleft [Ca^{2+}]. Under these conditions, only voltage-dependent processes dictated the inactivation rate of $I_{Ca,L}$; here sorcin *enhanced* the inactivation of $I_{Ca,L}$, i.e., the opposite effect to that seen when Ca^{2+}-dependent inactivation was present. This is similar to the effects observed by Meyers and co-workers [7] who used EGTA-containing pipette solutions. Under these circumstances, free [Ca^{2+}] within the cell would be very much lower, thereby reducing the influence of Ca^{2+}-dependent inactivation allowing voltage-dependant inactivation to dominate over Ca^{2+}-dependent inactivation. Therefore, the data by Meyers et al. [7] that appear at first sight to the opposite of those reported in this study, can be explained by the effects of sorcin on voltage-dependent inactivation. Similar effects of sorcin were observed when Ba^{2+} was used as the charge carrier; this reinforces the conclusion that sorcin has a distinct action on the LTCC in the absence of Ca^{2+}-dependent inactivation, i.e., when voltage-dependent alone determines the rate of inactivation. This latter result also indicates that sorcin does not require Ca^{2+} influx to mediate its effects. However, in the absence of intracellular Ca^{2+} (<1 nM, 10 mM BAPTA), addition of sorcin did not affect inactivation, indicating that diastolic Ca^{2+} levels (~150 nM) are sufficient to mediate sorcin's Ca^{2+}-sensitive actions. Only one binding site for sorcin has been demonstrated in the C-terminal region of α_{1C} subunit. The site at residues 1,622–2,171 overlaps with the CaM-binding domain [4]. The consequences of sorcin binding at this site on the activity of the LTCC have yet to be elucidated.

Sorcin's modulation of the LTCC as the sum of two independent effects

The data presented in this study indicates that sorcin influences both Ca^{2+}-dependent and voltage-dependent inactivation processes. The interrelationship between these two actions is unclear. While voltage-dependent inactivation can be studied in the absence of Ca^{2+}-dependent inactivation, the opposite is not true.

A number of different models could be used to account for sorcin's bifunctional modulatory influence on $I_{Ca,L}$. One model may be the exclusive influence of sorcin on Ca^{2+}-dependent and voltage-dependent inactivation separately with different Ca^{2+}-dependent thresholds. However, if it is assumed that both mechanisms normally operate simultaneously to determine the rate of inactivation of $I_{Ca,L}$, then under control conditions, the net effect of sorcin is the sum of both Ca^{2+}-dependent and voltage-dependent inactivation effects. Using this assumption, the effects on Ca^{2+}-dependent inactivation alone can be estimated by subtraction as shown in Table 1 for both sorcin and SCBD. The slowing of inactivation of $I_{Ca,L}$ by sorcin is a consequence of a larger effect on Ca^{2+}-dependant inactivation than voltage-dependent. On inhibition of the SR, the absence of any effect of sorcin on $I_{Ca,L}$ inactivation rate reflects a smaller effect of sorcin on Ca^{2+}-dependent inactivation which balances the effects on voltage-dependent inactivation. Further work is required on the molecular basis of sorcin's action on LTCC to verify the independent nature of the effects on Ca^{2+}-dependent and voltage-dependent inactivation.

Effect of raising extracellular Ca^{2+} after SR inhibition

As described above, the absence of any significant effect of sorcin after SR inhibition may be due to a smaller effect of

Table 1 Analysis of effects of sorcin and SCBD on $I_{Ca,L}$ inactivation

Effect	Relative change in the rate constant of inactivation (RC)	Relative change in the rate constant of inactivation (RC)
Effect in EGTA: a balance of effects on CDI and VDI ($E_{CDI\&VDI}$) E_{Sorc}=RC[sorcin]/RC[control]	RC [control]=0.114 ms^{-1} RC [Sorcin]= 0.067 ms^{-1} E_{sorc}=0.58=$E_{CDI\&VDI}$	RC [control]=0.114 ms^{-1} RC [SCBD]= 0.105 ms^{-1} E_{SCBD}=0.92=$E_{CDI\&VDI}$
Effect in BAPTA: an effect on VDI alone (E_{VDI}) E_{VDI}=RC[sorcin]/RC[control]	RC [control]=0.025 ms^{-1} RC [Sorcin]= 0.032 ms^{-1} E_{VDI}=1.28	RC [control]=0.025 ms^{-1} RC [SCBD]= 0.098 ms^{-1} EVDI=3.92
Effect on CDI (alone): E_{CDI}=$E_{CDI\&VDI}/E_{VDI}$	E_{CDI}=0.46	E_{CDI}=0.23
Effect in EGTA with SR block: (Thapsigargin) E_{Sorc}= RC[sorcin]/RC[control]	RC [control]=0.044 ms^{-1} RC [Sorcin]= 0.045 ms^{-1} E_{Sor}=1.02	
Effect on CDI with SR block: E_{CDI}=$E_{CDI\&VDI}/E_{VDI}$	E_{CDI}=0.78	

sorcin on Ca^{2+}-dependent inactivation (Table 1). To test this hypothesis, extracellular [Ca^{2+}] was increased after SR inhibition to try and increase Ca^{2+} influx, restore the cleft Ca^{2+} signal, and therefore the rate of Ca^{2+}-dependent inactivation. While the rate of inactivation was restored too close to control conditions (Fig. 3c), sorcin had no significant effects The reasons why this manipulation did not restore sorcin's effects on inactivation is unclear but may be related to complex effects of raising extracellular [Ca^{2+}] on surface charge, as well as current flow [24, 25] and may therefore not replicate the changes in cleft Ca^{2+} that occur when the SR is functional.

Possible mechanisms of action of sorcin on CDI

Sorcin may modulate Ca^{2+}-dependent inactivation by reducing the transient rise of [Ca^{2+}] in the cleft. This could be achieved by several mechanisms: (1) sorcin may modulate [Ca^{2+}] within the cleft by reducing the open probability of RyR2. However, previous studies have shown that manipulations to reduce RyR2 activity will only cause a transient reduction of SR Ca^{2+} release; no effects are observed in the steady state as SR Ca^{2+} content, and consequently, SR Ca^{2+} release increases back to control values [26]. (2) Ca^{2+}-dependent inactivation may also be slowed by sorcin buffering [Ca^{2+}] in the junctional cleft. Simplistically, this appears unlikely since only an additional 3 μM sorcin was added to the cytosol and concentrations ~1,000 times this value (i.e., ~3 mM) or more would be required to buffer cleft Ca^{2+} sufficiently to slow Ca^{2+}-dependent inactivation. There may be mechanisms to concentrate sorcin within the cleft, and certainly, the expression pattern of sorcin observed in isolated myocytes suggests preferential binding in the T-tubule area [3]. (3) sorcin may reduce the affinity of the Ca^{2+}-binding site on the cytoplasmic domain of the α_{1C}-subunit of the LTCC, but this possibility remains to be investigated.

Possible mechanisms of action of sorcin on VDI

The data concerning the effects of sorcin on voltage-dependent inactivation is similar to that previously reported for $I_{Ca,L}$ currents measured in *Xenopus* oocytes [7]. In this expression system, Ca^{2+}-dependent inactivation would not be expected to operate, and therefore, the measurements made in the oocyte expression system are comparable to measurements made in adult myocytes with BAPTA or using Ba^{2+} as a charge carrier. This study is also the first to provide evidence that endogenous sorcin has a tonic effect on the rate of inactivation of $I_{Ca,L}$. Down-regulation using an RNAi strategy caused a slowing of CII/VDI using BAPTA pipette solutions suggesting a tonic influence of endogenous protein on CII/VDI. It would be anticipated that endogenous sorcin would also affect CDI, but this was not tested in the current study.

The molecular mechanism underlying this effect is unclear; di-hydropyridine (DHP) agonists such as Bay-K-8644 cause enhanced inactivation by a shift in single channel gating in favor of longer single channel open times without alteration to channel amplitude (mode two gating) [27, 28]. Alternatively, stimulation of the β-adrenergic pathway causes a more negative shift in the current–voltage relationship and alters the CII/VDI in a similar fashion to sorcin [29, 29]. This is also thought to be due to a shift in single channel gating to one with longer open times and hence higher open probability [30]. Measurements on single channel currents would provide an insight into sorcin's molecular mechanisms.

The effect of SCBD

Our data describing the effect of the SCBD on $I_{Ca,L}$ inactivation finds no significant effect when compared to control currents. However, an enhancement of inactivation kinetics is revealed when Ca^{2+}-dependent inactivation is diminished in the presence of BAPTA. The SCBD data suggests that, like the sorcin–RyR2 interaction [20], that with the α-subunit is also via interaction with the C-terminal of sorcin. The lack of the normal N-terminal region appears to enhance the effect of the protein, implying that the N-terminal region may exert a mild inhibitory influence.

Involvement of phosphorylation pathways

Phosphorylation of α_{1C} by CaMKII and PKA are important physiological modulators of $I_{Ca,L}$, underlying the response to alterations in stimulation rate and β-adrenergic stimulation [24, 31–33]. The current study used the phenomenon of frequency-dependent facilitation (FDF) as an assay for CaMKII activity. Inhibition of CaMKinase II abolished FDF but not the action of sorcin, nor was inhibition of PKA effective in blocking sorcin's action on the inactivation of $I_{Ca,L}$. Since these pathways can also act to phosphorylate sorcin directly [9], the data indicates that phosphorylation of sorcin is not an essential step, despite previous reports to the contrary [34].

Physiological role of sorcin within the Ca^{2+} microdomain

Under physiological conditions, sorcin would be expected to tonically influence Ca^{2+}-dependent inactivation via changes in Ca^{2+} within the microdomain of the dyadic cleft. This action would be in parallel with the direct influence of Ca^{2+} on LTCC, the net result of which would be to endow Ca^{2+}-dependent inactivation with an extra degree of cooperation. However, this influence on $I_{Ca,L}$

cannot be considered in isolation since the documented inhibitory action of sorcin on RyR2 [5, 6] and the stimulatory action on NCX [6, 8] will also contribute to the final cleft Ca^{2+} signal. In doing so, sorcin endows the LTCC, NCX, and RyR2 within the microdomain with a Ca^{2+}-dependence that these proteins would not possess outside this region. This Ca^{2+}-dependence would be dictated by the Ca^{2+} affinity and kinetics of Ca^{2+} binding to sorcin in response to the transient nature of the cleft Ca^{2+} signal. Preliminary data indicate that sorcin levels may be altered in heart failure [35]; this would be anticipated to influence E–C coupling by changing the Ca^{2+} dependence of LTCC, RyR2, and NCX within the cleft.

Acknowledgements The authors would like to thank Aileen Rankin and June Irvine for preparation of cardiomyocytes. This work was funded by the British Heart Foundation (Mark Fowler and Godfrey Smith) and the Deutsche Forschungsgemeinschaft (DFG, grant 1233/7-3 (Gerd Hasenfuß and Tim Seidler); the authors would also like to thank Carlotta Zamparelli and Daniela Verzili for help in generation and purification of recombinant proteins.

References

1. Meyers MB, Spengler BA, Chang T-D, Melera PW, Biedler JL (1985) Gene amplification-associated cytogenic aberrations and protein changes in vincristine-resistant Chinese hamster, mouse and human cells. J Cell Biol 100:588–597
2. Van der Bliek AM, Meyers MB, Biedler JL, Hes E, Borst P (1986) A 22-kd protein (sorcin/V19) encoded by an amplified gene in multidrug-resistant cells, is homologous to the calcium-binding light chain of calpain. EMBO J 5:3201–3208
3. Meyers MB, Pickel VM, Sheu S-S, Sharma VK, Scotto KW, Fishmann GI (1995) Association of sorcin with the cardiac ryanodine receptor. J Biol Chem 270:26411–26418
4. Meyers MB, Puri TS, Chien AJ, Gao T, Hsu P-H, Hosey M, Fishmann GI (1998) Sorcin associates with the pore-forming subunit of voltage-dependent L-type Ca^{2+} channels. J Biol Chem 273:18930–18935
5. Farrell EF, Antaramian A, Rueda A, Gomez AM, Valdivia HH (2003) Sorcin inhibits calcium release and modulates excitation–contraction coupling in the heart. J Biol Chem 278(36):34660–34666
6. Siedler T, Miller SLW, Loughery CM, Kanie A, Burow A, Kettlewell S, Teucher N, Wagner S, Kogler H, Meyers MB, Hasenfuss G, Smith GL (2003) Effects of adenovirus-mediated sorcin overexpression on excitation–contraction coupling in isolated rabbit cardiomyocytes. Circ Res 93:132–139
7. Meyers MB, Fischer A, Sun J-Y, Lopes CMB, Rohacs T, Nakamura TY, Zhou Y-Y, Lee PC, Altschuld RA, McCune SA, Coetzee WA, Fishman GI (2003) Sorcin regulates excitation–contraction coupling in the heart. J Biol Chem 278(31):28865–28871
8. Collis LP, Meyers MB, Zhang J, Phoon CKL, Sobie EA, Coetzee WA, Fishmann GI (2007) Expression of a sorcin missense mutation in the heart modulates excitation–contraction coupling. FASEB J 21:475–487
9. Matsumoto T, Hisamatsu Y, Ohkusa T, Inoue N, Sato T, Suzuki S, Ikeda Y, Matsuzaki M (2005) Sorcin interacts with sarcoplasmic reticulum Ca^{2+}-ATPase and modulates excitation–contraction coupling in the heart. Basic Res Cardiol 100:1–13
10. Franzini-Armstrong C, Protasi F, Ramesh V (1999) Shape size and distribution of Ca^{2+} release units and couplons in skeletal and cardiac muscle. Biophys J 77:1528–1539
11. Gathercole DV, Colling DJ, Skepper JN, Takagishi Y, Levi AJ, Severs N (2000) Immunogold-labelled L-type calcium channels are clustered in the surface plasma membrane overlying junctional sarcoplasmic reticulum in guinea-pig myocytes—implications for excitation–contraction coupling in cardiac muscle. J Mol Cell Cardiol 32:1981–1994
12. Langer GA, Peskoff A (1996) Calcium concentration and movement in the dyadic cleft space of the cardiac ventricular cell. Biophys J 70:1169–1182
13. Eckert R, Chad JE (1984) Inactivation of Ca channels. Prog Biophys and Mol Biol 44:215–267
14. Hadley RW, Lederer WJ (1991) Ca^{2+} and voltage inactivate Ca^{2+} channels in guinea-pig ventricular myocytes through independent mechanisms. J Physiol 444:257–268
15. Sham JSK, Cleeman L, Morad M (1995) Functional coupling of Ca^{2+} channels and ryanodine receptors in cardiac myocytes. PNAS 92:121–125
16. Pott C, Yip M, Goldhaber JI, Philipson KD (2007) Regulation of cardiac L-type Ca^{2+} current in Na^{+}–Ca^{2+} exchanger knockout mice: Functional coupling of the Ca^{2+} channel and the Na^{+}-Ca^{2+} exchanger. Biophys J 92:1431–1437
17. McIntosh MA, Cobbe SM, Smith GL (2000) Heterogeneous changes in action potential and intracellular Ca^{2+} in left ventricular myocyte sub-types from rabbits with heart failure. Cardiovasc Res 45:397–409
18. Duncan L, Burton FL, Smith GL (1999) REACT: calculation of free metal and ligand concentrations using a Windows-based computer program. J Physiol 517P (Abstract)
19. Richard S, Tiaho F, Charnet P, Nargeot J, Nerbonne JM (1990) Two pathways for Ca^{2+} channel gating differentially modulated by physiological stimuli. Am J Physiol 27:H1872–H1881
20. Colotti G, Zamparelli C, Verzili D, Mella M, Loughery CM, Smith GL, Chiancone E (2006) The W105G and W99G sorcin mutants demonstrate the role of the D helix in the Ca^{2+}-dependent interaction with annexin VII and the cardiac ryanodine receptor. Biochem 45:12519–12529
21. Soeller C, Cannell MB (2004) Analysing cardiac excitation–contraction coupling with mathematical models of local control. Prog Biophys Mol Biol 85:141–162
22. Naraghi M, Neher E (1997) Linearized buffered Ca^{2+} diffusion in microdomains and its implications for calculation of [Ca^{2+}] at the mouth of a calcium channel. J Neurosci 17:6961–6973
23. Yuan W, Bers DM (1994) Ca-dependent facilitation of cardiac Ca current is due to Ca-calmodulin-dependent protein kinase. Am J Physiol 267:H982–H993
24. Hess P, Lansman JB, Tsien RW (1986) Calcium channel selectivity for divalent and monovalent cations; voltage and concentration dependence of single channel current in ventricular heart cells. J Gen Physiol 80:293–319
25. Guia A, Stern MD, Lakatta EG, Josephson IR (2001) Ion concentration-dependence of rat unitary L-type calcium channel conductance. Biophys J 80:2742–2750
26. Eisner DA, Trafford AW, Diaz ME, Overend CL, O'Neil SC (1998) The control of Ca release from the cardiac sarcoplasmic reticulum: regulation versus autoregulation. Cardiovasc Res 38:589–604
27. Hess P, Lansman JB, Tsien RW (1984) Different modes of Ca channel gating behaviour favoured by dihydropyridine Ca agonists and antagonists. Nature 311:538–544
28. Noceti F, Olcese R, Qin N, Zhou J, Stefani E (1998) Effect of Bay K 8644 (−) and the b_{2a} subunit on Ca^{2+}-dependnet inactivation in a_{1c} Ca^{2+} channels. J Gen Physiol 111:463–475
29. Bracken N, Elkadri M, Hart G, Hussain M (2006) The role of constitutive PKA-mediated phosphorylation in the regulation of

basal I_{Ca} in isolated rat cardiac myocytes. Br J Pharm 148:1108–1115
30. Yue DT, Herzig S, Marban E (1990) b-adrenergic stimulation of calcium channels occurs by potentiation of high-activity gating modes. PNAS 87:753–757
31. Schroder F, Herzig S (1999) Effects of b_2-adrenergic stimulation on single-channel gating of rat cardiac L-type Ca^{2+} channels. Am J Physiol 276:H834–H843
32. Tiaho F, Piot C, Nargeot J, Richard S (1994) Regulation of the frequency-dependent facilitation of L-type Ca^{2+} currents in rat ventricular myocytes. J Physiol 477:237–252
33. Findlay I (2002) b-adrenergic stimulation modulates Ca^{2+} and voltage-dependent inactivation of L-type Ca^{2+} channel currents in guinea-pig ventricular myocytes. J Physiol 541: 741–751
34. Lokuta AJ, Meyers MB, Sander PR, Fishman GI, Valdivia HH (1997) Modulation of cardiac ryanodine receptors by sorcin. J Biol Chem 272:25333–25338
35. Smith GL, Elliott EE, Kettlewell S, Curries S, Quinn FR (2006) Na(+)/Ca(2+) exchanger expression and function in a rabbit model of myocardial infarction. J Cardiovasc Electrophys 17: S57–S63